Response to the Editor - tc-2020-317

Dear Editor,

Please find a tracked-changes version of the manuscript tc-2020-317 attached below. Added text is displayed as blue underlined text, while removed text is displayed as red strike-through.

The modifications correspond to the detailed responses to the reviewers, uploaded on the discussion page of the manuscript. We have reported the main ones (not pertaining to typos or direct reformulations) below in *highlighted italics*, alongside our reasoning behind the proposed modifications. The line numbers are based on the tracked-changes version.

L1: We clarified the first sentence to indicate that heat conduction and vapor transport are usually treated as decoupled (in response to review 2).
"Heat transport in snowpacks is understood to occur through the two processes of heat conduction and latent heat transport carried by water vapor, which are generally treated as decoupled from one another. "

L9: We specified that our work only covers heat and mass transport in snow (in response to review 1).
"[…] could be a reasonable assumption for modeling heat and mass transfer in snow."

L38: We clarified that one of our goal is to study the coupling between heat conduction and vapor transport at the macroscopic scale (in response to review 2).
"The aim of this article is to provide a simplified analysis of the contribution of latent heat to the thermal energy flux in snow, and notably to quantify the coupling between these processes at the macroscopic scale.*"*

L45: We specified that the absence of convection is a simplifying assumption (in response to review 1).
"We also make the simplifying assumption that convection in the pore space does not occur or can be neglected (similarly to Riche and Schneebeli, 2013 or Calonne et al., 2014)."

L65: We provided an example under which the macroscopic vapor flux is no longer proportional to the macroscopic vapor gradient (in response to review 1).
"[…] depending on the nature of the mechanisms at play at the microscopic scale (for instance in the case of a dependence of the sticking coefficient of water molecules onto ice on the local saturation of water vapor, as discussed in Fourteau et al., 2021)."

L68: We clarified that we consider that snow is transverse orthotropic (in response to review 3).
"However, snow can be considered as a transverse isotropic material (e.g., Löwe et al., 2013), and this tensor is thus fully characterized [...] "

L97: We specified that we work under the assumption of Temperature Gradient metamorphism (in response to review 1).
"Finally, when a sufficiently large thermal gradient is imposed on a snow sample, the variations of c_{sat} due to differences in curvature of the ice surface become negligible compared to variations due to temperature differences (Colbeck, 1983). This large temperature gradient condition, corresponds to the regime of Temperature Gradient metamorphism, usually observed for thermal gradients of 10 K m^{-1} and above (Sommerfeld and LaChappelle, 1970, Colbeck, 1982)."

L126: We clarified that in the slow kinetics case, there is not enough release and absorption of latent heat to meaningfully impact the snow temperature (in response to review 1).
"A macroscopic vapor flux might be present, but there is simply not enough mass than changes phase and release/absorption of latent heat to meaningfully impact the heat flux in the snow"

L132: We specified that in the case of fast kinetics, the Hertz Knudsen equation is replaced by the saturation of water vapor (in response to review 3).
"[…] and the Hertz-Knudsen equation is replaced by the saturation of vapor at the ice/air interface."

L160: We specified how the averaged temperature gradients are defined (in response to review 1).
"Note that the average thermal gradient in the ice (respectively the air) is defined by performing the volume average in the ice space only (respectively the air space only), and not in the entire snow volume."

L179: We recalled how Jordan (1991) and Sturm and Johnson (1992) derived the decomposition of the total heat flux in a purely conduction part and a latent heat part (in response to review 1).
"[…] has notably been reported by Jordan (1991) and Sturm and Johnson (1992), by directly considering energy balance and transport at the macroscopic scale and pre-supposing the existence of well-defined (i.e. independent of the macroscopic thermal gradient) K^{cond} and D^{eff}."

L187: We specified how the presence of vapor and latent heat impact the thermal contrast between the phases, and their individual averaged thermal gradients (in response to review 1).
"The presence of latent heat increases the apparent thermal conductivity of the pore space, and thus reduces the thermal conductivity contrast between the two phases. In turn, this reduced thermal contrast increases the average temperature gradient [...]"

L216: We specified that the relation given in Figure 2 corresponds to the upper-boundary of effective water vapor diffusion coefficient (in response to review 1).
"Moreover, as the macroscopic vapor flux decreases with slower kinetics (Pinzer et al., 2012, Fourteau et al., 2021), this curve represents an upper limit for the effective diffusion coefficient."

L214: We specified how the macroscopic heat flux is numerically computed and specified that the choice of the macroscopic thermal gradient used in the simulation is arbitrary and does not impact our results (in response to review 1).
"The macroscopic heat flux Q is computed as the volume average of the microscopic heat fluxes using the Paraview software. Note that the chosen value of 50 $K\ m^{-1}$ for the imposed gradient is purely arbitrary and does not impact our results, as the resulting effective thermal conductivity does not depend on the magnitude of the gradient.""

L247: We provided a reference to the Clausius-Clapeyron equation (in response to review 1).
"[…] by assuming that water vapor follows the Clausius-Clapeyron and ideal gas laws (Eq. 11 in Fourteau et al., 2021)"

L271: We reformulated the sentence describing the origin of the temperature dependence of the effective thermal conductivity (in response to review 1).
"The temperature dependence of K^{eff} is due to the temperature dependence of the underlying materials. Indeed, an increasing temperature results in the decrease of the ice thermal conductivity k_i and the increase of the apparent thermal conductivity of the air k_v due to both the increase [...]"

L281: Equation 17 is now an equation of his own (in response to review 3).

L283: We specified how K^{cond}, K^{ice} and K^{air} are computed (in response to review 1).
"With our simulations, the values of K^{cond}, K^{ice}, K^{air} are computed directly from K^{eff}, k_i, k_a, and k_v, and using Equations 11 and 12."

Figure 8: We clarified the meaning of the symbols in the caption of Figure 8 (in response to review 3).
*"**Figure 8.** Effective thermal conductivity of snow as a function of density, under the fast kinetics assumption at 263K. The horizontal bar of a symbol marks the horizontal effective thermal conductivity value of a snow sample, while the tip of the vertical bar marks its vertical value."*

L361: We proposed a way to extend our effective thermal conductivity parametrization to other temperatures (in response to review 3).
"This parametrization can be extended to other temperatures by first computing the thermal conductivity at the desired density for the 5 proposed temperatures and then performing an interpolation to the desired temperature."

L365: We clarified that the slopes of the effective thermal conductivity against density curves are decreasing with increasing temperature (in response to review 3).
"[…] show a decrease of the slopes of the thermal conductivity versus density curves with increasing temperatures."

L393: We clarified why the bias reported for the needle probe method should not impact the general trend of the temperature dependence of the effective thermal conductivity (in response to review 3).
"Even though recent studies have highlighted a potential bias of the needle probe method when used with snow (Calonne et al., 2011; Riche and Schneebeli, 2013), this reported bias does not impact the trend of thermal conductivity measured at different temperature in similar snow samples, as performed by Sturn and Johnson (1992). These data can thus be expected to reflect the variation of the effective thermal conductivity with temperature."

L397: We specified that the slow kinetics hypothesis cannot explain the observed temperature dependence of the effective thermal conductivity (in response to reviews 2 and 3).
"These measurements, displayed in Figure 7 of Sturm and Johnson (1992), clearly indicate an exponential-like increase of thermal conductivity with temperature, consistent with the fast kinetics hypothesis but not with the slow kinetics hypothesis."

L400: We clarify that we are referring to the measurements of Sokratov and Maneo (2000) (in response to review 1).
"While direct measurements of the effective diffusion coefficient are difficult and should therefore be analyzed with caution, the reported experimental values of Sokratov and Maeno (2000) reports an average normalized diffusion coefficient of 0.64 for snow densities of [...]"

L410: We clarified while the fast kinetics assumption is in agreement with the available experimental data, the overall validity of this assumption still need to be backed by more data. Moreover, the development of macroscopic heat and mass transport theoretical model, applicable to arbitrary kinetics, would be welcomed, and should be compared to the fast kinetics assumption in order to select the best hypothesis for heat and mass modeling in snowpacks (in response to reviews 2 and 3).
"All the above reasons suggest that the effective thermal conductivity and diffusion coefficient of water vapor in snow could be well represented under the fast kinetics hypothesis, at least during temperature gradient metamorphism. Further experimental work should be performed to confirm that the fast kinetics assumption generally applies for modeling mass and heat transport in snow and to highlight its potential limitations. Also, the derivation of a theoretical model able to describe

heat and mass transfer with arbitrary surface kinetics would allow to investigate intermediate kinetics, in an effort to ultimately select the best modeling assumptions for snow. At the same time, this model could be formulated to explicitly take into account macroscopic convection, as this phenomenon has been observed in sub-artic shallow snowpacks (Trabant and Benson, 1972, Sturm and Johnson, 1991). Its derivation could be achieved using standard homogenization methods, such the as two-scale asymptotic expansion (e.g. Municchi and Icardi, 2020) or volume averaging methods (e.g. Whitaker, 1977).”

L434: The article of Moyne et al. (1988) does not treat humid soils per se, but humid tri-phasic media in general.
“A similar conclusion was reached by Moyne et al. (1988) for the thermal conductivity of humid tri-phasic medium.”

L460: We specified that our conclusion only applies to heat and mass transport and under temperature gradient metamorphism conditions (in response to review 1).
“This suggests that the fast kinetics option might be well suited to model heat and mass transport in snow during temperature gradient metamorphism.”

Best Regards,
Kévin Fourteau on behalf of all co-authors

Impact of water vapor diffusion and latent heat on the effective thermal conductivity of snow

Kévin Fourteau[1], Florent Domine[2,3], and Pascal Hagenmuller[1]

[1]Univ. Grenoble Alpes, Université de Toulouse, Météo-France, CNRS, CNRM, Centre d'Études de la Neige, Grenoble, France

[2]Takuvik Joint International Laboratory, Université Laval (Canada) and CNRS-INSU (France), Québec, QC, G1V 0A6, Canada

[3]Centre d'Études Nordiques (CEN) and Department of Chemistry, Université Laval, Québec, QC, G1V 0A6, Canada

Correspondence: kfourteau@protonmail.com

Abstract. Heat transport in snowpacks is ~~generally thought~~ understood to occur through ~~two independent processes :~~ the two processes of heat conduction and latent heat transport carried by water vapor, which are generally treated as decoupled from one another. This paper investigates the coupling between both these processes in snow, with an emphasis on the impacts of the kinetics of the sublimation and deposition of water vapor onto ice. In the case where kinetics is fast, latent heat exchanges at ice surfaces modify their temperature, and therefore the thermal gradient within ice crystals and the heat conduction through the entire microstructure. Furthermore, in this case, the effective thermal conductivity of snow can be expressed by a purely conductive term complemented by a term directly proportional to the effective diffusion coefficient of water vapor in snow, which illustrates the inextricable coupling between heat conduction and water vapor transport. Numerical simulations on measured three-dimensional snow microstructures reveal that the effective thermal conductivity of snow can be significantly larger, by up to about 50 % for low-density snow, than if water vapor transport is neglected. Comparison of our numerical simulations with literature data suggests that the fast kinetics hypothesis could be a reasonable assumption ~~to model snowphysical properties~~for modeling heat and mass transport in snow. Lastly, we demonstrate that under the fast kinetics hypothesis the effective diffusion coefficient of water vapor is related to the effective thermal conductivity by a simple linear relationship. Under such condition, the effective diffusion coefficient of water vapor is expected to lie in the narrow 100 % to about 80 % range of the value of the diffusion coefficient of water vapor in air for most seasonal snows. This may greatly facilitate the parameterization of water vapor diffusion of snow in models.

1 Introduction

Thermal conductivity is one of the major physical properties of snow. It governs the magnitude of the thermal energy flux through the snowpack when subjected to a thermal gradient, and thus plays an integral role in the energy budgets of the ground (Zhang et al., 1996), ice caps and glaciers (Gilbert et al., 2012), sea ice (Lecomte et al., 2013), as well as in the temperature of the snow surface and therefore in meteorology (Domine et al., 2019). Moreover, variations of thermal conductivity between snow layers impact the temperature gradients at the layer scale, and thus in part ~~governs~~ govern snow metamorphism (Vionnet et al., 2012). In light of its importance for the understanding of snow and environmental physics, snow thermal conductivity has been actively studied and measured for several decades (Yosida et al., 1955; Jaafar and Picot, 1970; Sturm and Johnson, 1992; Morin et al., 2010; Calonne et al., 2011; Riche and Schneebeli, 2013; Domine et al., 2015).

One of the peculiarities of snow is that energy transport does not solely occur through heat conduction. Indeed, when a snowpack is subjected to a thermal gradient, a macroscopic water vapor flux is also present (Sturm and Benson, 1997; Pinzer et al., 2012). This vapor flux carries latent heat, in parallel to heat conduction. Several studies have investigated the influence of vapor transport on the total energy flux through snow under a thermal gradient. Among others, Sturm and Johnson (1992) report that the heat transport in snow is characterized by an effective thermal conductivity $\mathbf{K}^{\mathrm{eff}}$ encompassing both the effects of heat conduction and vapor transport. In their framework, one can decompose the effective thermal conductivity as $\mathbf{K}^{\mathrm{eff}} = \mathbf{K}^{\mathrm{cond}} + \mathbf{K}^{\mathrm{vap}}$, where $\mathbf{K}^{\mathrm{cond}}$ is *"the hypothetical conductivity in the absence of any vapor transport"* (Sturm and Johnson, 1992) and $\mathbf{K}^{\mathrm{vap}}$ corresponds to the latent heat transported with water vapor. In opposition to the idea of merging conduction and vapor tansport in a single effective thermal conductivity, Calonne et al. (2011) *"recommend purely conductive effects (i.e. conduction through ice and interstitial air) to be considered separately from non-conductive processes"*, therefore treating heat conduction as decoupled from vapor transport.

The aim of this article is to provide a simplified analysis of the contribution of latent heat to the thermal energy flux in snow, and notably to quantify to what degree heat conduction can or cannot be decoupled from latent heat and vapor transportnotably to quantify the coupling between these processes at the macroscopic scale. For this we focus on two limiting cases, considering the kinetics of deposition and sublimation of water vapor to be either very fast or very slow. We start by providing theoretical considerations on the relationship between water vapor transport and the effective thermal conductivity. We then perform numerical simulations to quantify the contribution of latent heat to the effective thermal conductivity.

2 Theory

Let us consider a snow sample of volume V, subjected to a macroscopic thermal gradient denoted ∇T^{M} (potentially accompanied by a macroscopic vapor concentration gradient ∇C^{M})and in the absence of . We also make the simplifying assumption that convection in the pore space does not occur or can be neglected (similarly to Riche and Schneebeli, 2013; Calonne et al., 2014) . Furthermore, let us assume that the sample is taken large enough to be larger than its Representative Elementary Volume (REV; Auriault et al., 2010; Calonne et al., 2014). Moreover, we assume that the sample is small enough that it does not span several snow layers, and that the macroscopic thermal and water vapor gradients can be considered constant over the sample. Under these conditions, the volume V of snow is representative of the entire snow layer, and both share the same physical properties. The existence of this intermediate size between the microscopic and macroscopic scales is guaranteed by the separation of scales between the microscopic and macroscopic descriptions, which is a necessary condition to treat snow as an equivalent homogeneous medium with well defined physical properties (Auriault, 1991; Auriault et al., 2010). An illustration of the microscopic and macroscopic points of view and of the separation of scale between them is given in Figure 1.

Table 1. Symbols and definitions of the major variables used in this article. The convention followed is that a tensorial variable is denoted with a bold capitalized letter, and its scalar components with the non-bold capitalized letter.

Symbol	Definition
$\mathbf{K}^{\mathrm{eff}}$	Effective thermal conductivity of snow
$K^{\mathrm{eff}}_{\mathrm{xy}}$	Horizontal component of the effective thermal conductivity of snow
$K^{\mathrm{eff}}_{\mathrm{z}}$	Vertical component of the effective thermal conductivity of snow
K^{eff}	Scalar component of the effective thermal conductivity of snow (either horizontal or vertical)
$\mathbf{K}^{\mathrm{cond}}$	Purely conductive part of the thermal conductivity of snow
$\mathbf{K}^{\mathrm{vap}}$	Vapor transport part of the thermal conductivity of snow
K^{air}	Contribution of air heat conduction to the vertical effective thermal conductivity of snow (Equation 16)
K^{ice}	Contribution of ice heat conduction to the vertical effective thermal conductivity of snow (Equation 16)
$\mathbf{D}^{\mathrm{eff}}$	Effective diffusion coefficient of water vapor in snow
$D^{\mathrm{eff}}_{\mathrm{xy}}$	Horizontal component of the effective diffusion coefficient of water vapor in snow
$D^{\mathrm{eff}}_{\mathrm{z}}$	Vertical component of the effective diffusion coefficient of water vapor in snow
D^{eff}	Scalar component of the effective diffusion coefficient of water vapor in snow (either horizontal or vertical)
$\mathbf{D}^{\mathrm{norm}}$	Normalized effective diffusion coefficient of water vapor in snow
D_0	Diffusion coefficient of water vapor in air
$\cdot_{\mathrm{slow}}$	Subscript pertaining to the slow kinetics hypothesis
$\cdot_{\mathrm{fast}}$	Subscript pertaining to the fast kinetics hypothesis
β	Derivative of the saturated water vapor concentration with respect to temperature, $\beta = \frac{dc_{\mathrm{sat}}}{dT}$
L	Latent heat of sublimation of ice
k_{i}	Thermal conductivity of ice
k_{a}	Thermal conductivity of air
k_{v}	Apparent thermal conductivity of air, $k_{\mathrm{v}} = k_{\mathrm{a}} + \beta L D_0$

The effective thermal conductivity $\mathbf{K}^{\mathrm{eff}}$ of snow relates the macroscopic heat flux Q, transporting thermal energy at the macroscopic scale, to the thermal gradient ∇T^{M} with $Q = -\mathbf{K}^{\mathrm{eff}} \nabla T^{\mathrm{M}}$ (e.g. Yosida et al., 1955; Sturm and Johnson, 1992; Riche and Schneebeli, 2013). Similarly, an effective vapor diffusion coefficient $\mathbf{D}^{\mathrm{eff}}$ can be defined, which relates the macro-

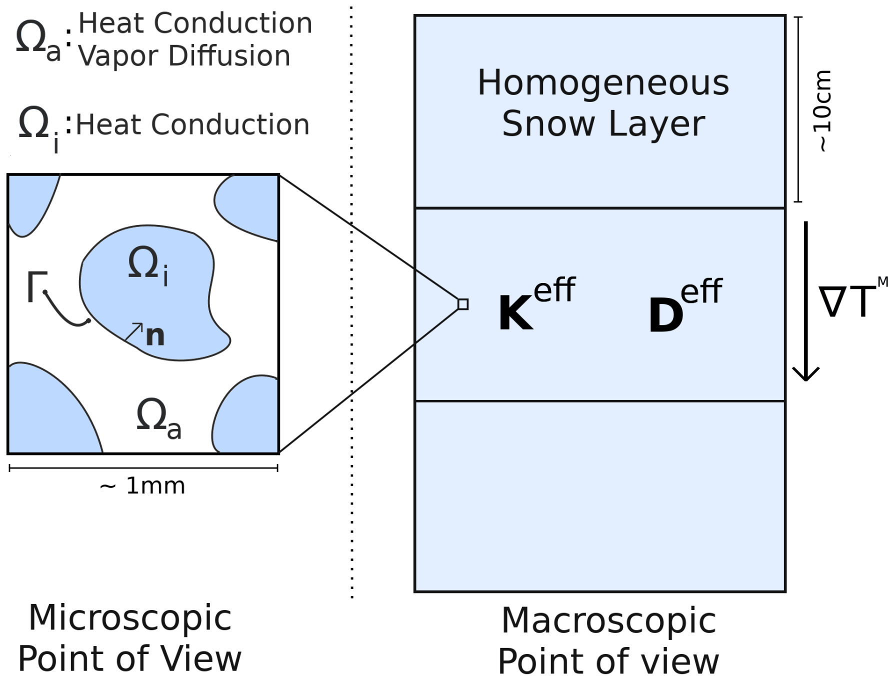

Figure 1. Illustration of the microscopic and macroscopic points of view of snow. At the microscopic scale, snow is composed of an ice space (Ω_i) and a pore space (Ω_a), separated by a boundary (Γ). Heat conduction occurs through the ice and pore spaces, while vapor diffusion is limited to the pore space. At the macroscopic scale, snow is treated as an equivalent homogeneous medium, with an effective thermal conductivity $\mathbf{K}^\mathrm{eff}$ and an effective water vapor diffusion coefficient $\mathbf{D}^\mathrm{eff}$, and is subjected to a macroscopic thermal gradient ∇T^M.

scopic vapor flux F to the macroscopic concentration gradient ∇C^M with $F = -\mathbf{D}^\mathrm{eff}\nabla C^\mathrm{M}$ (e.g. Shertzer and Adams, 2018; Fourteau et al., 2021). In snow sciences, it is usually expected that the effective thermal conductivity and vapor diffusion coefficient ~~only depends~~ depends only on the snow microstructure and on the physical properties of the underlying materials (the ice and the air), but not on the macroscopic thermal and water vapor concentration gradients (Yosida et al., 1955; Jaafar and Picot, 1970; Sturm and Johnson, 1992; Colbeck, 1993; Morin et al., 2010; Calonne et al., 2011; Riche and Schneebeli, 2013; Domine et al., 2015). One should however keep in mind that it might not necessarily be true, depending on the nature of the mechanisms at play at the microscopic scale ~~(Fourteau et al., 2021)~~(for instance in the case of a dependence of the sticking coefficient of water molecules onto ice on the local saturation of water vapor, as discussed in Fourteau et al. (2021))

Finally, the effective thermal conductivity is represented by a 3×3 tensor. However, ~~due to the transversal anisotropy of snow~~ snow can be considered as a transverse isotropic material (Löwe et al., 2013), and this tensor is thus fully characterized by two scalar values, namely the vertical and horizontal thermal conductivities. These scalar values are respectively denoted $K_\mathrm{z}^\mathrm{eff}$ and $K_\mathrm{xy}^\mathrm{eff}$ in this article, to differentiate them from the tensor. Similarly, $\mathbf{D}^\mathrm{eff}$ is represented by a 3×3 tensor, but for snow it reduces to ~~a~~ vertical and a horizontal components. Again, these scalar components are respectively denoted $D_\mathrm{z}^\mathrm{eff}$ and $D_\mathrm{xy}^\mathrm{eff}$. We define the normalized effective diffusion coefficient $\mathbf{D}^\mathrm{norm}$ as $\mathbf{D}^\mathrm{norm} = \mathbf{D}^\mathrm{eff}/D_0$, where D_0 is the diffusion coefficient of water vapor in air. The definitions and symbols of the variables used for this work are summarized in Table 1.

In this article, the effective thermal conductivity of snow will be obtained starting from the physics at the microscopic scale. The relevant microscopic physical mechanisms for heat transport are (i) heat conduction in the ice, (ii) heat conduction in the air, (iii) vapor diffusion in the air (iv) vapor deposition/sublimation at ice surfaces (Calonne et al., 2014). Moreover, we assume that the physics at the microscopic scale can be treated in a steady state. From our understanding this is justified as the time scale governing the microscopic scale is much shorter than the macroscopic time scale, at which snow observations are made. Indeed, Hansen and Foslien (2015) report that the characteristic times at the macroscopic and microscopic scales differ by a ~~10^6 factor~~ factor of 10^6. Consistent with this, Calonne et al. (2014) report that when expressed in a non-dimensional form, the time derivatives in the heat and mass equations are negligible compared to the flux terms. The microscopic equations governing energy and vapor transport are thus

$$\begin{cases} \mathrm{div}(-k_\mathrm{i}\nabla T_\mathrm{i}) = 0 & (\Omega_\mathrm{i}) \\ \mathrm{div}(-k_\mathrm{a}\nabla T_\mathrm{a}) = 0 & (\Omega_\mathrm{a}) \\ \mathrm{div}(-D_0\nabla c) = 0 & (\Omega_\mathrm{a}) \\ T_\mathrm{i} = T_\mathrm{a} & (\Gamma) \\ -k_\mathrm{i}\nabla T_\mathrm{i}\cdot\mathbf{n} = -k_\mathrm{a}\nabla T_\mathrm{a}\cdot\mathbf{n} - LD_0\nabla c\cdot\mathbf{n} & (\Gamma) \\ -D_0\nabla c\cdot\mathbf{n} = \alpha v_\mathrm{kin}(c - c_\mathrm{sat}) & (\Gamma) \end{cases} \tag{1}$$

where Ω_i, Ω_a, Γ, and $\mathbf{n}$ represent the ice space, the pore space, the ice/pore interface, and the normal vector to Γ pointing toward the ice, respectively. The geometry of the microscopic problem is exemplified in Figure 1. k_i and k_a are the thermal conductivities of ice and air, T_i and T_a are the ice and air temperatures, D_0 is the diffusion coefficient of vapor in the air, c is the concentration of vapor in the pores, c_sat is the saturation concentration of vapor at the ice interface, L is the latent heat of sublimation of ice, $v_\mathrm{kin} = \sqrt{(kT)/(2\pi m)}$ is referred to as the kinetic velocity and is related to the velocity of water molecules in the gas phase (with k the Boltzmann's constant and m the mass of a water molecule), and α is a coefficient less than or equal to unity referred to as the sticking coefficient (or sometimes the accommodation coefficient) of water vapor molecules on ice surfaces. The last equation of the system is referred to as the Hertz-Knudsen equation and governs the sublimation and deposition of water molecules on the ice surfaces (Saito, 1996). The penultimate equation, represents the impact of vapor sublimation/deposition on the continuity of the heat flux at the ice/pore interface. Finally, when a sufficiently large thermal gradient is imposed ~~to~~ on a snow sample, the variations of c_sat due to differences in curvature of the ice surface become negligible compared to variations due to temperature differences (Colbeck, 1983). ~~Thus in~~ This large temperature gradient condition, corresponds to the regime of Temperature Gradient metamorphism, usually observed for thermal gradients of $10\,\mathrm{K\,m^{-1}}$ and above (Sommerfeld and LaChapelle, 1970; Colbeck, 1982). In this case, the saturation concentration of vapor can be treated as a function of the ice surface temperature only.

The system of Equations 1 shows that there exists a two-way coupling between heat and vapor transport in snow. Indeed, the ice and air temperatures are impacted by the phase change of water vapor and the release/absorption of latent heat, while the water vapor concentration in the pores is impacted by temperature through the value of c_{sat} at the ice surfaces. This implies that the heat flux through a snow sample depends on the sublimation and deposition processes happening in the snow, and that the magnitude of the coupling between the heat flux and the vapor transport depends on the kinetics of the adsorption and desorption of water molecules. This kinetics is encapsulated in the parameter α of the Hertz-Knudsen equation. A general treatment of the system of Equations 1 in the case of an arbitrary α is however out of the scope of this article. In this work, we limit ourselves to two limiting cases, namely very slow (small α) and very fast (large α) surface kinetics. Moreover, we only focus on quantifying the energy and water vapor fluxes and their associated effective thermal conductivity and effective diffusion coefficient of vapor, without deriving the complete macroscopic temperature and vapor equations (contrary to the work of Calonne et al., 2014, for instance). Finally, note that the notion of slow and fast kinetics is related to the notion of kinetics-limited (small α) and diffusion-limited (large α) metamorphism in snow (e.g. Krol and Löwe, 2016).

2.1 The slow kinetics case

In the slow kinetics case, we consider that α is sufficiently small that the sublimation/deposition of water vapor does not strongly impact the temperature field in the snow microstructure. In this case, the coupling between heat and water vapor can be neglected, and snow can be viewed as an inert medium for heat conduction. This slow kinetics case has been treated in ~~details~~ detail by Calonne et al. (2011) and the case 3 of Calonne et al. (2014). Here, the snow sample is characterized by an effective thermal conductivity $\mathbf{K}^{\mathrm{eff}}_{\mathrm{slow}}$ that only accounts for the heat conduction through the ice and the air, as if the snow medium were inert for water vapor. The subscript slow, used in $\mathbf{K}^{\mathrm{eff}}_{\mathrm{slow}}$ and elsewhere in the paper, is used to emphasize the slow kinetics assumption. Calonne et al. (2011) showed that the effective thermal conductivity depends on the snow microstructure and on the ice and air thermal conductivities, but not on the macroscopic thermal gradient. It can be obtained with microscale numerical simulations of heat conduction, which do not include vapor transport (e.g. Calonne et al., 2011; Riche and Schneebeli, 2013). Following a similar decomposition of the effective conductivity as that reported by Sturm and Johnson (1992), one has $\mathbf{K}^{\mathrm{eff}}_{\mathrm{slow}} = \mathbf{K}^{\mathrm{cond}}_{\mathrm{slow}}$ and $\mathbf{K}^{\mathrm{vap}}_{\mathrm{slow}} = 0$. Note that the fact that $\mathbf{K}^{\mathrm{vap}}_{\mathrm{slow}} = 0$ does not imply that the vapor flux in snow is null. A macroscopic vapor flux might be present, but there is simply not enough ~~sublimation and deposition to~~ mass that changes phase and release/absorption of latent heat to meaningfully impact the heat flux in the snow.

2.2 The fast kinetics case

In the fast kinetics case, α is sufficiently large that the adsorption/desorption of water molecules is fast enough to impose vapor saturation at the ice/air interface. Mathematically, this case can be treated by letting $\alpha \to \infty$. While this mathetimatically treatment is purely theoretical (as $\alpha \leq 1$), it helps in apprehending the effect of fast kinetics. This case corresponds to the diffusion-limited case, and the Hertz-Knudsen equation ~~reduces to~~ is replaced by the saturation of vapor at the ice~~surface~~/air interface. Moreover, it can be shown that in this case the vapor concentration equals its saturation value not only at the ice surface, but also throughout the entire pore space (see Yosida et al. (1955) or Fourteau et al. (2021) for demonstrations). The system of Equations 1 can therefore be rewritten as

$$\begin{cases} \mathrm{div}(-k_{\mathrm{i}}\nabla T_{\mathrm{i}}) = 0 \qquad (\Omega_{\mathrm{i}}) \\ \mathrm{div}(-k_{\mathrm{a}}\nabla T_{\mathrm{a}}) = 0 \qquad (\Omega_{\mathrm{a}}) \\ \mathrm{div}(-D_0\nabla c_{\mathrm{sat}}) = 0 \qquad (\Omega_{\mathrm{a}}) \\ T_{\mathrm{i}} = T_{\mathrm{a}} \qquad (\Gamma) \\ -k_{\mathrm{i}}\nabla T_{\mathrm{i}}\cdot\mathbf{n} = -k_{\mathrm{a}}\nabla T_{\mathrm{a}}\cdot\mathbf{n} - LD_0\nabla c_{\mathrm{sat}}\cdot\mathbf{n} \qquad (\Gamma) \end{cases} \tag{2}$$

Using the chain rule one has $\nabla c_{\mathrm{sat}} = \beta\nabla T_{\mathrm{a}}$, where $\beta = \frac{dc_{\mathrm{sat}}}{dT}$. Re-injecting this equality in Equations 2 yields

$$\begin{cases} \mathrm{div}(-k_{\mathrm{i}}\nabla T_{\mathrm{i}}) = 0 \qquad (\Omega_{\mathrm{i}}) \\ \mathrm{div}(-k_{\mathrm{a}}\nabla T_{\mathrm{a}}) = 0 \qquad (\Omega_{\mathrm{a}}) \\ \mathrm{div}(-\beta D_0\nabla T_{\mathrm{a}}) = 0 \qquad (\Omega_{\mathrm{a}}) \\ T_{\mathrm{i}} = T_{\mathrm{a}} \qquad (\Gamma) \\ -k_{\mathrm{i}}\nabla T_{\mathrm{i}}\cdot\mathbf{n} = -k_{\mathrm{a}}\nabla T_{\mathrm{a}}\cdot\mathbf{n} - \beta LD_0\nabla T_{\mathrm{a}}\cdot\mathbf{n} \qquad (\Gamma) \end{cases} \tag{3}$$

Multiplying the third line by L and summing with the second line, one finally gets

$$\begin{cases} \mathrm{div}(-k_{\mathrm{i}}\nabla T_{\mathrm{i}}) = 0 \qquad (\Omega_{\mathrm{i}}) \\ \mathrm{div}(-(k_{\mathrm{a}} + \beta LD_0)\nabla T_{\mathrm{a}}) = 0 \qquad (\Omega_{\mathrm{a}}) \\ T_{\mathrm{i}} = T_{\mathrm{a}} \qquad (\Gamma) \\ -k_{\mathrm{i}}\nabla T_{\mathrm{i}}\cdot\mathbf{n} = -(k_{\mathrm{a}} + \beta LD_0)\nabla T_{\mathrm{a}}\cdot\mathbf{n} \qquad (\Gamma) \end{cases} \tag{4}$$

which is the system of equations governing the temperature and heat conduction in a microstructure without any explicit vapor transport and where the conductivity of the air has been replaced by an apparent conductivity k_{v}, defined as

$$k_{\mathrm{v}} = k_{\mathrm{a}} + \beta LD_0 \tag{5}$$

An equivalent demonstration of this result was proposed by Yosida et al. (1955). A similar result was also derived by Moyne et al. (1988) for a tri-phasic medium, composed of water vapor, liquid water, and an inert solid phase, and is consistent with the effective thermal conducitivty model of soil proposed by De Vries (1958) and De Vries (1987).

As this system of Equations is equivalent to the one of an inert medium with an increased air thermal conductivity, one can show using methods of homogenization (e.g. Auriault et al., 2010; Calonne et al., 2011) that at the macroscopic scale snow can be treated as an equivalent medium with a well-defined tensorial thermal conductivity $\mathbf{K}^{\mathrm{eff}}_{\mathrm{fast}}$. This effective thermal conductivity depends on the snow microstructure and on the physical properties of ice, air, and vapor (through k_i, k_a, and $\beta L D_0$), but not on the macroscopic thermal gradient. Again, the subscript fast is used to stress out that we are working under the fast kinetics assumption.

We now investigate the individual contributions of conduction and vapor transport to $\mathbf{K}^{\mathrm{eff}}_{\mathrm{fast}}$. The macroscopic heat flux Q, which equals the volume average of the microscopic heat flux (Batchelor and Brien, 1977), can be decomposed as

$$\begin{aligned} Q &= -\frac{1}{V}\Big(\int_{V_\mathrm{i}} k_\mathrm{i}\nabla T_\mathrm{i}\mathrm{d}V + \int_{V_\mathrm{a}} k_\mathrm{v}\nabla T_\mathrm{a}\mathrm{d}V\Big) \\ &= -(1-\phi)\frac{1}{V_\mathrm{i}}\int_{V_\mathrm{i}} k_\mathrm{i}\nabla T_\mathrm{i}\mathrm{d}V - \phi\frac{1}{V_\mathrm{a}}\int_{V_\mathrm{a}} k_\mathrm{a}\nabla T_\mathrm{a}\mathrm{d}V - \phi\frac{1}{V_\mathrm{a}}\int_{V_\mathrm{a}} \beta L D_0\nabla T_\mathrm{a}\mathrm{d}V \\ &= -(1-\phi)k_\mathrm{i} < \nabla T_\mathrm{i} > -\phi k_\mathrm{a} < \nabla T_\mathrm{a} > -\phi\beta L D_0 < \nabla T_\mathrm{a} > \end{aligned} \qquad (6)$$

where V_i and V_a are the ice and air volumes in the snow, ϕ is the porosity, and $< \nabla T_\mathrm{i} >$ and $< \nabla T_\mathrm{a} >$ stand for the spatial averages of the thermal gradients in the individual ice and air spaces. Note that the average thermal gradient in the ice (respectively the air) is defined by performing the volume average in the ice space only (respectively the air space only), and not in the entire snow volume. The first two terms of the last line of Equation 6 respectively correspond to the contribution of ice and air heat conduction to the energy flux, while the last term corresponds to an additional contribution of latent heat transported with water vapor. Moreover, recalling that with fast kinetics $\nabla c = \nabla c_\mathrm{sat} = \beta\nabla T_\mathrm{a}$, the contribution of water vapor is given by

$$\begin{aligned} \phi\beta L D_0 < \nabla T_\mathrm{a} > &= L\frac{1}{V}\int_{V_\mathrm{a}} \beta D_0\nabla T_\mathrm{a}\,\mathrm{d}V \\ &= L\frac{1}{V}\int_{V_\mathrm{a}} D_0\nabla c\,\mathrm{d}V \\ &= LF \end{aligned} \qquad (7)$$

where $F = \frac{1}{V}\int_{V_\mathrm{a}} D_0\nabla c\,\mathrm{d}V$ is the macroscopic vapor flux (Shertzer and Adams, 2018; Fourteau et al., 2021) which is linked to the macroscopic vapor gradient ∇C^M through an effective diffusion coefficient $\mathbf{D}^{\mathrm{eff}}_{\mathrm{fast}}$, such that $F = -\mathbf{D}^{\mathrm{eff}}_{\mathrm{fast}}\nabla C^\mathrm{M}$ (Calonne et al., 2014; Fourteau et al., 2021). Since in the fast kinetics case vapor is at saturation throughout the pore space, the macroscopic vapor gradient is related to the macroscopic temperature gradient ∇T^{M} by $\nabla C^{\mathrm{M}} = \beta \nabla T^{\mathrm{M}}$. Therefore, the macroscopic vapor flux is given by

$$F = -\beta \mathbf{D}_{\mathrm{fast}}^{\mathrm{eff}} \nabla T^{\mathrm{M}} \tag{8}$$

The effective thermal conductivity of snow can thus be decomposed in

$$\mathbf{K}_{\mathrm{fast}}^{\mathrm{eff}} = \mathbf{K}_{\mathrm{fast}}^{\mathrm{cond}} + \beta L \mathbf{D}_{\mathrm{fast}}^{\mathrm{eff}} \tag{9}$$

where $\mathbf{K}_{\mathrm{fast}}^{\mathrm{cond}}$ is the contribution due to heat conduction in the ice and air, and $\beta L \mathbf{D}_{\mathrm{fast}}^{\mathrm{eff}} = \mathbf{K}_{\mathrm{fast}}^{\mathrm{vap}}$ is the contribution of latent heat transported with water vapor. Contrary to the slow kinetics case, we now find that latent heat impacts the thermal properties of snow, and that the vapor flux directly contributes to the effective thermal conductivity. A similar version of Equation 9, with the contribution of vapor transport being $\beta L \mathbf{D}_{\mathrm{fast}}^{\mathrm{eff}}$, has notably been reported by Jordan (1991) or Sturm and Johnson (1992), by directly considering energy balance and transport at the macroscopic scale and pre-supposing the existence of well-defined (i.e. independent of the macroscopic thermal gradient) K^{cond} and D^{eff}.

It is important to note that $\mathbf{K}_{\mathrm{fast}}^{\mathrm{cond}}$ in Equation 9 is different from the thermal conductivity when latent heat effects are neglected, i.e. $\mathbf{K}_{\mathrm{fast}}^{\mathrm{cond}} \neq \mathbf{K}_{\mathrm{slow}}^{\mathrm{cond}}$ (Moyne et al., 1988). Indeed, the heat conduction in the microstructure is determined by the distribution of the local thermal gradients in the two phases, and latent heat modifies the microscopic thermal gradients compared to the case without latent heat, and thus modifies the heat conduction. The presence of latent heat increases the apparent thermal conductivity of the pore space, and thus reduces the thermal conductivity contrast between the two phases. ~~This~~ In turn, this reduced thermal contrast increases the average temperature gradient of the ice phase (the highly conducting phase) and decreases the average temperature gradient of the gas phase (the poorly conducting phase). The increase of heat conduction in the ice is larger than the decrease in the air, and the contribution of heat conduction alone is therefore greater with the presence of latent heat than without. Such an effect is illustrated and quantified with numerical simulations ~~is~~ in Section 3.1.

Finally, we want to point out that in the fast kinetics case, the effective thermal conductivity and the effective water vapor diffusion coefficient are linearly related. Indeed, starting from the fact that the effective diffusion coefficient is given by the ratio of the magnitude of the vapor flux over the magnitude of the vapor concentration gradient, one has

$$D_{\mathrm{fast}}^{\mathrm{eff}} = \frac{\|\frac{1}{V}\int_{V_{\mathrm{a}}} D_0 \nabla c \,\mathrm{d}V\|}{\|\nabla C\|} = \frac{\|D_0 \beta \frac{1}{V}\int_{V_{\mathrm{a}}} \nabla T_{\mathrm{a}} \,\mathrm{d}V\|}{\|\beta \nabla T^{\mathrm{M}}\|} = D_0 \frac{V_{\mathrm{a}}}{V} \frac{\|\frac{1}{V_{\mathrm{a}}}\int_{V_{\mathrm{a}}} \nabla T_{\mathrm{a}} \,\mathrm{d}V\|}{\|\nabla T^{\mathrm{M}}\|} = D_0 \phi \frac{\| < \nabla T_{\mathrm{a}} > \|}{\|\nabla T^{\mathrm{M}}\|} \tag{10}$$

where we used the facts that $\nabla c = \beta \nabla T_{\mathrm{a}}$ and $\nabla C^{\mathrm{M}} = \beta \nabla T^{\mathrm{M}}$, and where $D_{\mathrm{fast}}^{\mathrm{eff}}$ either stands for the vertical or for the horizontal effective diffusion coefficient depending on the orientation of the macroscopic thermal gradient. The ratio of the average thermal gradient in the pore space over the macroscopic thermal gradient is governed by the effective thermal conductivity and the thermal conductivity of the ice and the air. Indeed, we have

$$K_{\mathrm{fast}}^{\mathrm{eff}} \nabla T^{\mathrm{M}} = (1-\phi) k_{\mathrm{i}} < \nabla T_{\mathrm{i}} > + \phi k_{\mathrm{v}} < \nabla T_{\mathrm{a}} > \tag{11}$$

and

$$\nabla T^{\mathrm{M}} = (1-\phi) < \nabla T_{\mathrm{i}} > + \phi < \nabla T_{\mathrm{a}} > \tag{12}$$

where similarly $K_{\mathrm{fast}}^{\mathrm{eff}}$ either stands for the vertical or for the horizontal effective thermal conductivity depending on the orientation of the macroscopic thermal gradient. Equation 11 follows from the definition of the macroscopic energy flux (Batchelor and Brien, 1977), and Equation 12 follows from the application of Stokes theorem and has notably been previously reported by Hansen and Foslien (2015). Combining Equations 11 and 12 we have that

$$\phi < \nabla T_{\mathrm{a}} > = \frac{k_{\mathrm{i}} - K_{\mathrm{fast}}^{\mathrm{eff}}}{k_{\mathrm{i}} - k_{\mathrm{v}}} \nabla T^{\mathrm{M}} \tag{13}$$

Finally, injecting Equation 13 in Equation 10 we have that

$$D_{\mathrm{fast}}^{\mathrm{eff}} = D_0 \frac{k_{\mathrm{i}} - K_{\mathrm{fast}}^{\mathrm{eff}}}{k_{\mathrm{i}} - k_{\mathrm{v}}} \tag{14}$$

Since the effective thermal conductivity is larger than the conductivity of the least conducting phase, i.e. $K_{\mathrm{fast}}^{\mathrm{eff}} > k_{\mathrm{v}}$, one finds that $D_{\mathrm{fast}}^{\mathrm{eff}} \leq D_0$, as reported by Giddings and LaChapelle (1962) and Fourteau et al. (2021). The linear relationship between the effective thermal conductivity and the normalized effective water vapor diffusion coefficient at $263\,\mathrm{K}$ is displayed in Figure 2, for effective thermal conductivities $\mathbf{K}_{\mathrm{fast}}^{\mathrm{eff}}$ ranging from $k_{\mathrm{v}} = 0.0336\,\mathrm{W\,K^{-1}\,m^{-1}}$ to $0.5\,\mathrm{W\,K^{-1}\,m^{-1}}$, as typically encountered with seasonal snow (e.g. Sturm et al., 1997; Calonne et al., 2011; Riche and Schneebeli, 2013, and the numerical values computed in Section 3.2 of this paper). Application of Equation 14 in Figure 2 reveals that the normalized effective diffusion coefficient ranges from 1 to about 0.8 for most seasonal snow. Moreover, as the macroscopic vapor flux decreases with slower kinetics (Pinzer et al., 2012; Fourteau et al., 2021), this curve represents an upper limit for the effective diffusion coefficient.

2.3 Intermediate cases

Numerous works indicate that α depends on temperature, the local vapor saturation, and the crystallographic properties of the underlying ice surface (e.g. Saito, 1996; Libbrecht and Rickerby, 2013), but for snow it remains unclear for snow what value or expression should be used for α in the Hertz-Knudsen Equation (Legagneux and Domine, 2005). However, a recent study

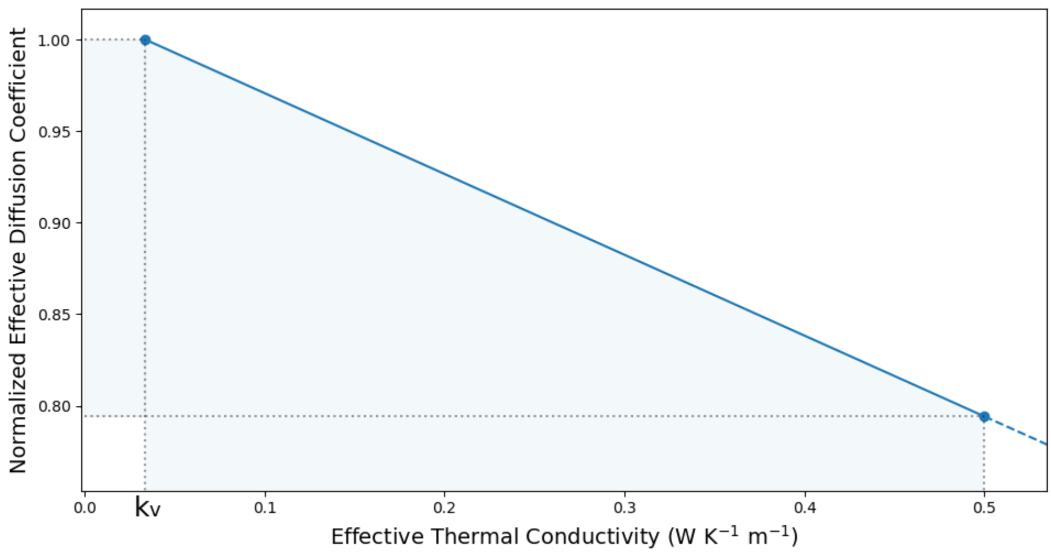

Figure 2. Normalized effective water vapor diffusion coefficient as a function of the effective thermal conductivity, under the fast kinetics hypothesis at $263\,\mathrm{K}$. The shaded area cover the typical range of thermal conductivity values (from k_v up to $0.5\,\mathrm{W\,K^{-1}\,m^{-1}}$) and the corresponding range of the normalized effective diffusion coefficient of water vapor (from 1 to about 0.8). At $263\,\mathrm{K}$, $k_\mathrm{v} = k_\mathrm{a} + \beta L D_0 = 0.0336\,\mathrm{W\,K^{-1}\,m^{-1}}$.

suggests that the very slow kinetics and fast surface kinetics cases ~~respectively~~ correspond to the minimum and maximum macroscopic vapor diffusion in snow, respectively (Fourteau et al., 2021). We can therefore expect the energy flux Q to be maximal in the fast kinetics case, since this corresponds to the situation with maximal vapor flux and the fastest adsorption and desorption of water molecules onto the ice surface. Similarly, the energy flux is minimal in the slow kinetics case as latent heat effects are absent in this case. The energy flux in snow Q can thus be bounded by the slow kinetics and the fast kinetics cases:

$$K^{\mathrm{eff}}_{\mathrm{slow}} \|\nabla T^{\mathrm{M}}\| \leq Q \leq K^{\mathrm{eff}}_{\mathrm{fast}} \|\nabla T^{\mathrm{M}}\| \tag{15}$$

where this inequality applies both for the vertical and horizontal components of the effective thermal conductivities, depending on the orientation of the macroscopic thermal gradient.

3 Numerical Simulations

To exemplify and quantify the points raised in Section 2, we performed Finite Element simulations of steady-state thermal conduction through several snow microstructures obtained experimentally with computed microtomography. The simulations were performed using the open source ElmerFEM software (Malinen and Råback, 2013), and the readily available solver for the heat equation.

In each simulation, the temperatures of two opposite sides of the microstructure were imposed in order to obtain a thermal gradient of $50\,\mathrm{K\,m^{-1}}$, with adiabatic conditions on the remaining sides. Similarly to Riche and Schneebeli (2013), the effective thermal conductivities are estimated by computing the ratio of the macroscopic heat flux Q to the macroscopic thermal gradient ∇T^{M}. The macroscopic heat flux Q is computed as the volume average of the microscopic heat fluxes using the Paraview software. Note that the chosen value of $50\,\mathrm{K\,m^{-1}}$ for the imposed gradient is purely arbitrary and does not impact our results, as the resulting effective thermal conductivity does not depend on the magnitude of the gradient.
In order to test the influence of temperature on the effective thermal conductivity of snow, the simulations were run for different mean temperatures, ranging from 223 to 273 K. The temperature dependence of the thermal conductivities of ice and air (k_{i} and k_{a}) were respectively taken from Lide (2006) (based on Slack, 1980) and Kadoya et al. (1985). The parameter $\beta = \frac{dc_{\mathrm{sat}}}{dT}$ was obtained by assuming that water vapor follows the Clausius-Clapeyron and ideal gas laws (Eq. 11 of Fourteau et al., 2021) . We set the diffusion coefficient of water vapor in air to $D_0 = 2 \times 10^{-5}\,\mathrm{m^2\,s^{-1}}$ (Calonne et al., 2014) and the latent heat of sublimation of ice $L = 28 \times 10^5\,\mathrm{J\,kg^{-1}}$ (Lide, 2006), independently of temperature. Finally, we assume that the density of ice ρ_{ice} is constant with temperature and equal to $917\,\mathrm{kg\,m^{-3}}$ (Calonne et al., 2014). The density of the samples reported in this article are computed using ρ_{ice} and the ice volume fraction deduced from the tomography images.
For the different microstructures and mean temperatures, two types of simulations were performed. One where we assumed no impact of latent heat on the heat conduction (thus obtaining $\mathbf{K}^{\mathrm{eff}}_{\mathrm{slow}}$), the other where we increased the apparent thermal conductivity of air by a $\beta L D_0$ term (thus obtaining $\mathbf{K}^{\mathrm{eff}}_{\mathrm{fast}}$). Moreover, as seen in Section 2.2 with Equation 14, under the fast kinetics assumption the effective diffusion coefficient of water vapor $\mathbf{D}^{\mathrm{eff}}_{\mathrm{fast}}$ can be directly obtained from the effective thermal conductivity. Finally, we recall that the normalized effective diffusion coefficient is defined as the ratio of the effective diffusion coefficient with the diffusion coefficient of water vapor in free air, i.e. $\mathbf{D}^{\mathrm{norm}} = \mathbf{D}^{\mathrm{eff}}/D_0$.

In total we used 34 measured snow microstructures, covering several types of seasonal snow. The particular snow types used are, according to the terminology of Fierz et al. (2009), precipitation particles (PP), decomposing and fragmented precipitation particles (DF), rounded grains (RG), faceted crystals (FC), depth hoar (DH), and melt forms (MF). We used sample sizes larger than the REV sizes reported by Calonne et al. (2011). The tetrahedral meshes used in the Finite Element simulations were produced using the CGAL library, and contains between 20 and 90 ~~millions of~~ million elements. The samples are described in the Supplementary Material, and includes both previously published snow samples (from Hagenmuller et al., 2016, 2019; Peinke et al., 2020) and new snow samples.

3.1 Effect of temperature on the effective thermal conductivity

In this section we analyze the influence of the mean temperature on the effective thermal conductivity. For simplicity, we limit ourselves to vertical temperature gradients, and thus only deal with vertical effective thermal conductivities and vertical diffusion coefficients of water vapor. As all scalar components are vertical, we do not use the subscript z, in order to lighten the notation.

~~Physically, the~~ The temperature dependence of K^{eff} is due to the ~~following causes, as temperature increases: (i)~~ temperature dependence of the underlying materials. Indeed, an increasing temperature results in the decrease of the ice thermal conductivity k_{i} ~~(ii)~~ and the increase of the apparent thermal conductivity of the air k_{v} due to both the increase of the intrinsic thermal conductivity of air k_{a} and the increase of the contribution of water vapor latent heat $\beta L D_0$, all displayed in Figure 3.

Furthermore, we define for our analysis

$$K^{\mathrm{ice}} = (1-\phi) k_{\mathrm{i}} \frac{\| < \nabla T_{\mathrm{i}} > \|}{\|\nabla T\|}$$
$$K^{\mathrm{air}} = \phi k_{\mathrm{a}} \frac{\| < \nabla T_{\mathrm{a}} > \|}{\|\nabla T\|} \tag{16}$$

K^{ice} (not to be mistaken with k_{i}, see Table 1) corresponds to the contribution of the ice heat conduction to the total effective thermal conductivity, and K^{air} (not to be mistaken with k_{a}) to the contribution of the air heat conduction. We have ~~$K^{\mathrm{cond}} = K^{\mathrm{ice}} + K^{\mathrm{air}}$,~~ by construction

$$K^{\mathrm{cond}} = K^{\mathrm{ice}} + K^{\mathrm{air}} \tag{17}$$

where K^{cond} is the vertical component of $\mathbf{K}^{\mathrm{cond}}$. With our simulations, the values of K^{cond}, K^{ice}, K^{air} are computed directly from K^{eff}, k_{i}, k_{a}, and k_{v}, and using Equations 11 and 12.

We first focus on only two snow samples, a low-density sample and a high-density sample. The low-density sample is composed of decomposing and fragmented precipitation particles (DF), with a density of $125\,\mathrm{kg\,m^{-3}}$ and a specific surface area of $40\,\mathrm{m^2\,kg^{-1}}$. The high-density sample is composed of melt forms (MF), with a density of $380\,\mathrm{kg\,m^{-3}}$ and a specific surface area of $5\,\mathrm{m^2\,kg^{-1}}$. The 3D microstructures of both samples are displayed in Figure 4. The results of the Finite Element simulations for these two samples are reported in Figure 5.

We start by analyzing the low-density sample (left column of Figure 5). Under the fast kinetics hypothesis, the effective thermal conductivity of the low-density sample shows an exponential-like increase with increasing temperature. This increase of K^{eff} is due to the combined effects of (i) an increase of K^{vap}, the vertical component of the contribution of latent heat transport and (ii) an increase of K^{cond}, the heat conduction through the ice and air spaces. The increase of K^{cond} is principally due to the increase of K^{ice}, the heat conduction in the ice. With increasing temperature, the increase of the apparent thermal conductivity of air reduces the contrast between the two phases and the average ice thermal gradient increases. This increase more than offsets the decrease of the ice thermal conductivity k_{i}, and the net effect is an increase of K^{ice}. Under the slow

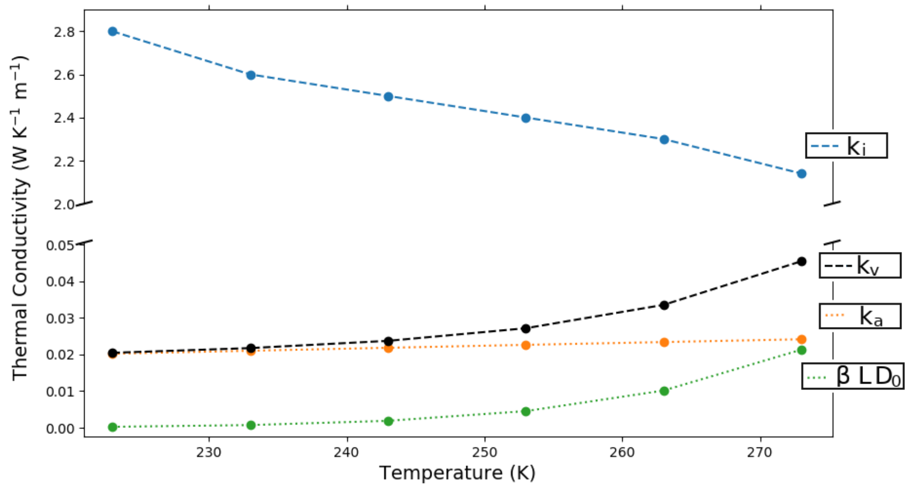

Figure 3. Temperature dependence of the thermal conductivity of ice (k_i in blue), of the thermal conductivity of air (k_a in orange), of the contribution of latent heat to the apparent thermal conductivity of the air ($\beta L D_0$ in green), and of the apparent thermal conductivity of air including latent heat effect ($k_\mathrm{v} = k_\mathrm{a} + \beta L D_0$ in black). Note the break in the y-axis.

kinetics hypothesis however, the effective thermal conductivity only barely decreases over the range of temperature studied, ~~consistently~~ consistent with the results of Calonne et al. (2011). In this case, the increase of the thermal conductivity of the air is not as pronounced, and the increase of the thermal gradient in the ice does not compensate for the decrease of the ice thermal conductivity. Overall K^ice decreases with temperature in the slow kinetics case.

Contrary to the low-density sample, the high-density sample (right column of Figure 5) shows a decrease of the effective thermal conductivity in the fast kinetics case. The increase of K^vap with temperature does not counter the decrease of K^cond. This decrease of K^cond can be attributed to the decrease of K^ice with temperature. Here, the increase of the ice thermal gradient is not large enough to offset the decrease of the ice thermal conductivity k_i, and overall K^ice decreases. Under the slow kinetics hypothesis, the effective thermal conductivity of the high-density sample decreases with temperature slightly more rapidly than in the fast kinetics case.

For both samples, the difference between $K^\mathrm{eff}_\mathrm{slow}$ and $K^\mathrm{eff}_\mathrm{fast}$ is maximal near the melting point, where it reaches more than 50% for low-density snow. Moreover, neglecting the effect of water vapor transport on heat conduction under the fast kinetics case can lead to an underestimation of about 20% of the conduction contribution. Thus in the fast kinetics case, the effect of latent heat can only reasonably be neglected for low temperatures or high-density samples.

In order to better quantify the difference between the fast and slow kinetics cases, we computed the vertical effective thermal conductivity for the totality of our 34 snow samples under both hypotheses, at 248 and 273 K. The ratios of the effective thermal

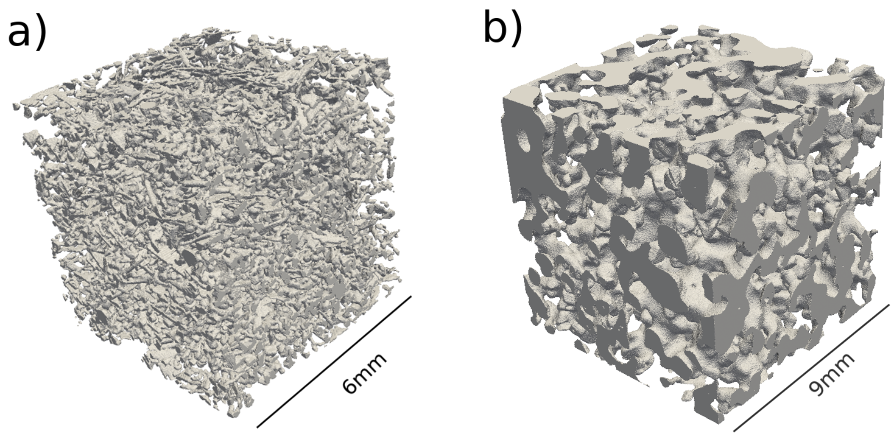

Figure 4. Tetrahedral meshes (ice phase only) of the low-density DF sample (panel a) and high-density MF sample (panel b).

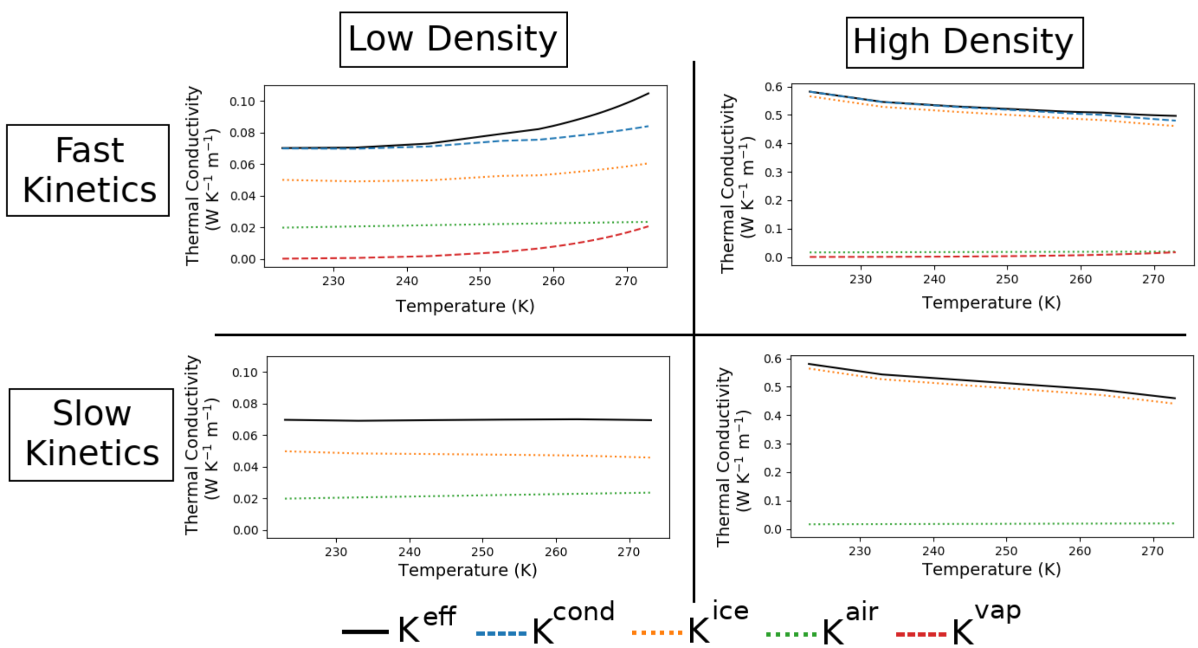

Figure 5. Vertical effective thermal conductivity (K^{eff}), with the contributions of ice heat conduction (K^{ice}), air heat conduction (K^{air}) and vapor transport (K^{vap}) for a low-density snow sample (left column) and a high-density snow sample (right column), and in the fast (upper line) and slow kinetics (lower line) cases. K^{cond} stands for the purely conductive part of K^{eff} and is given by $K^{\text{cond}} = K^{\text{ice}} + K^{\text{air}}$.

conductivity in the fast kinetics case over the slow kinetics case are displayed in Figure 6. They confirm that the relative difference is more important for low-density snow and for higher temperatures. Near the melting point (panel b), the fast kinetics effective thermal conductivity is between 10 to 50% higher than in the slow kinetics case. For colder snow at 248 K (panel a),

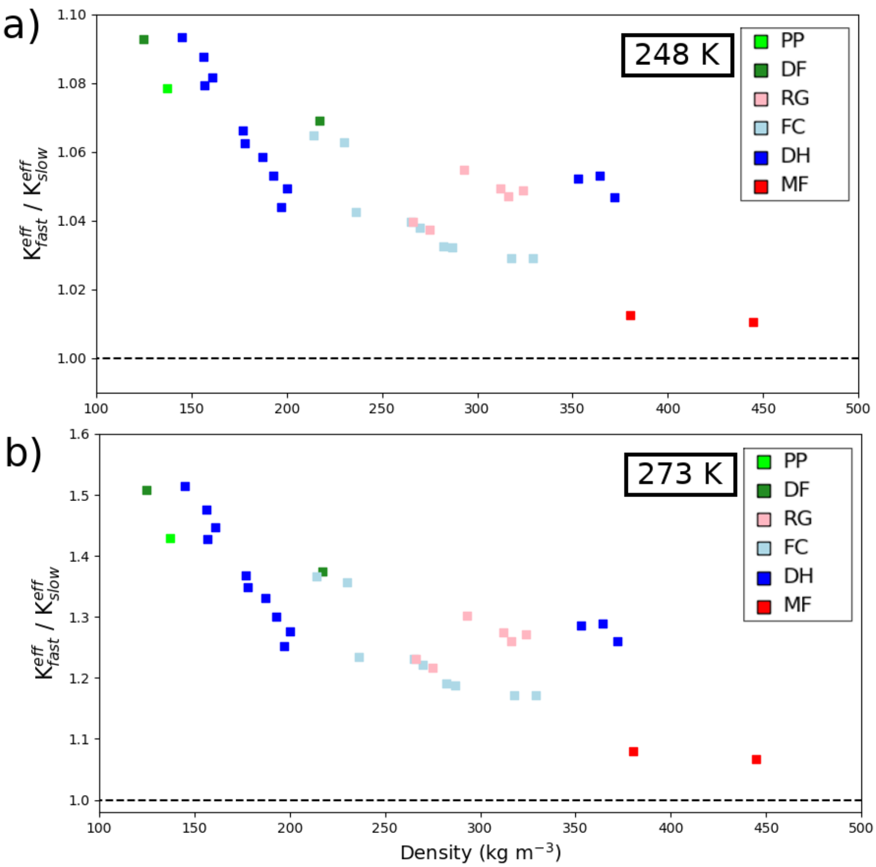

Figure 6. Ratio of the fast kinetics over the slow kinetics vertical effective thermal conductivity for various snow samples as a function of density. Computations performed at 248 K in panel a, and 273 K in panel b. Note the ~~difference~~ different y-scales in both panels.

the relative difference is less marked and ranges from 1 to 10%. When expressed in absolute terms, however, the difference between the fast and slow kinetics thermal conductivity is more marked for high-density snow.

Finally, Figure 7 shows the variation of the vertical normalized effective diffusion coefficient of water vapor with temperature, under the fast kinetics hypothesis and for the low and high-density samples shown in Figure 4. The numerical values are consistent with the recent study of Fourteau et al. (2021), who obtained effective diffusion coefficients using Finite Element simulations explicitly representing vapor diffusion in the pores. Figure 7 reveals a slight decrease of the effective diffusion coefficient with temperature, for both low and high-density snow. This can be explained by the decrease of the air thermal gradient, as the apparent conductivity of air increases with temperature. A lower air temperature gradient leads to a lower vapor

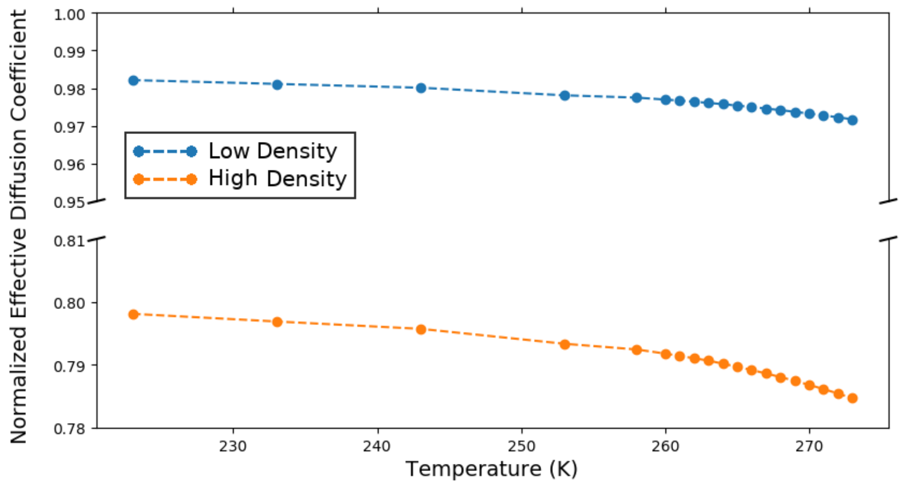

Figure 7. Vertical normalized effective diffusion coefficient $D_{\mathrm{fast}}^{\mathrm{norm}}$ of a low-density snow sample (blue) and a high-density snow sample (orange) as a function of temperature and under the hypothesis of fast kinetics. Note the break in the y-axis.

concentration gradient in the pores and thus to a lower vapor flux and a lower $D_{\mathrm{fast}}^{\mathrm{norm}}$.

3.2 Effective thermal conductivity and diffusion coefficient as a function of snow density

The slow kinetics effective thermal conductivities of snow samples covering a broad range of densities and microstructures have been reported by Calonne et al. (2011) and Riche and Schneebeli (2013). Similarly, numerical values of the effective diffusion coefficient of water vapor in snow under limited kinetics have been provided by Calonne et al. (2014). Here, we provide numerical estimates of the effective thermal conductivities and effective diffusion coefficients of a broad range of snow samples, this time under the fast kinetics hypothesis. For each sample we computed the vertical and horizontal effective thermal conductivities and water vapor effective diffusion coefficients, at 5 different temperatures (223, 248, 263, 268, and 273 K). The thermal conductivities and diffusion coefficients of each simulated sample are available in the Supplementary Material.

The thermal conductivities computed at 263 K are displayed in Figure 8 as a function of density. Similarly to the work of Calonne et al. (2011) and Riche and Schneebeli (2013) we observe that density and thermal conductivity are well correlated, with denser snow samples presenting higher thermal conductivity values. For the low-density samples, for which the conduction of air plays a determinant role in the effective thermal conductivity, we report thermal conductivity values higher than the polynomial fits of Calonne et al. (2011) and Riche and Schneebeli (2013), both based on the slow kinetics hypothesis. This difference can be explained by the increased apparent thermal conductivity of the air, due to latent heat effects. At higher density, our data lie above the reported data and polynomial fit of Calonne et al. (2011). As the relative difference between the fast and slow kinetics cases is small for high-density samples, one can expect the slow and fast kinetics simulations to yield

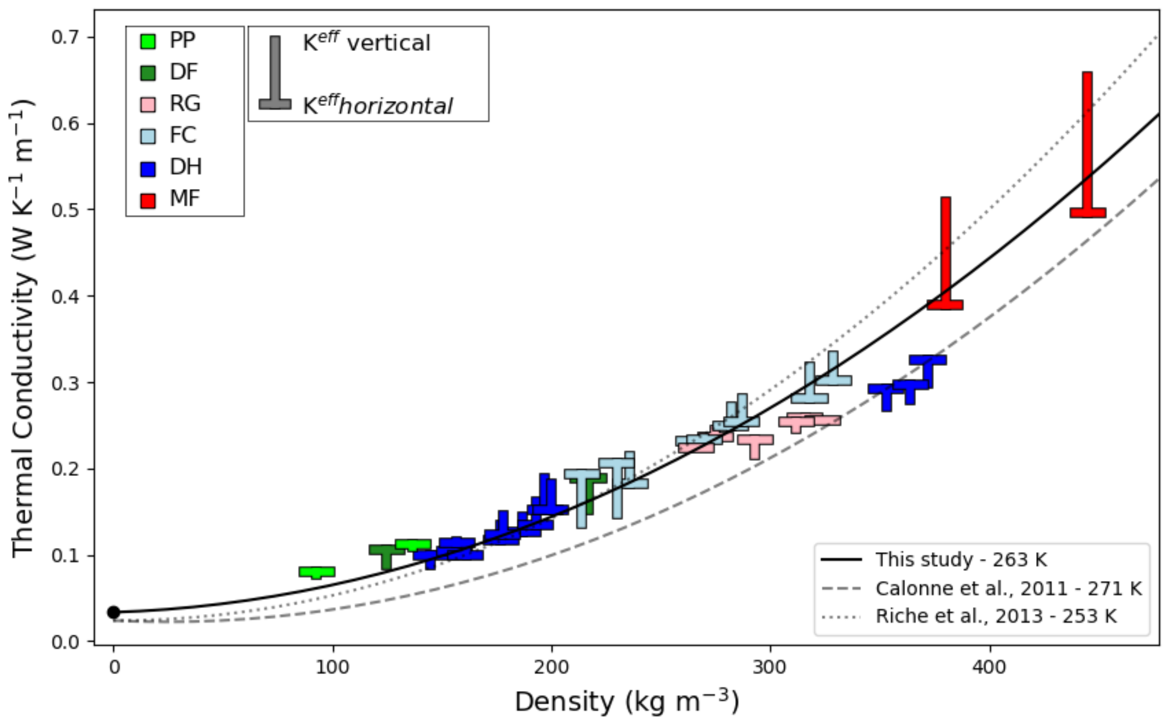

Figure 8. Effective thermal conductivity of snow as a function of density, under the fast kinetics assumption at 263 K. The horizontal bar of a symbol marks the horizontal effective thermal conductivity value of a snow sample, while the tip of the vertical bar marks its vertical value. Snow classification according to Fierz et al. (2009). Black dot: apparent thermal conductivity of air at 263 K. Solid black line: second order polynomial fit of the vertical effective thermal conductivity. Dashed grey line: polynomial fit proposed by Calonne et al. (2011), under the slow kinetics assumption at 271 K. Dotted grey line: polynomial fit proposed by Riche and Schneebeli (2013), under the slow kinetics assumption at 253 K.

similar values for high-density samples. The scatter between our values and the study of Calonne et al. (2011) is likely due to the inherent variability between snow samples, even for equal densities. Note that the fit proposed by Riche and Schneebeli (2013) was based on faceted crystals and depth hoar snow only, and at 253 K. On the contrary the fit proposed by Calonne et al. (2011) was based on their entire sample set at 271 K.

We adjusted second order polynomial functions to derive parametrizations of thermal conductivity as a function of density, and this for each of the 5 temperatures studied. Our parametrization for the vertical effective thermal conductivity at 263 K

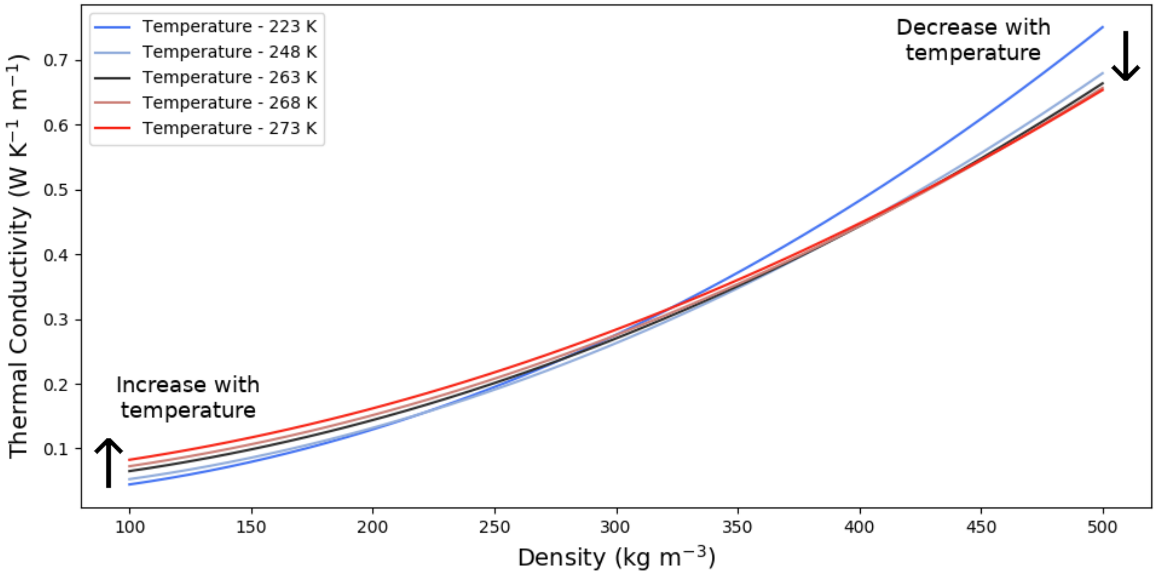

Figure 9. Temperature dependence of the vertical effective thermal conductivity parametrizations under the fast kinetics hypothesis.

is displayed as a solid line in Figure 8. The parametrizations of the vertical effective thermal conductivity for the 5 different temperatures are given by

$$K_z^{\text{eff}} = \begin{cases} 2.564\left(\frac{\rho}{\rho_{\text{ice}}}\right)^2 - 0.059\frac{\rho}{\rho_{\text{ice}}} + 0.0205 & \text{for T = 223 K} \\ 2.172\left(\frac{\rho}{\rho_{\text{ice}}}\right)^2 + 0.015\frac{\rho}{\rho_{\text{ice}}} + 0.0252 & \text{for T = 248 K} \\ 1.985\left(\frac{\rho}{\rho_{\text{ice}}}\right)^2 + 0.073\frac{\rho}{\rho_{\text{ice}}} + 0.0336 & \text{for T = 263 K} \\ 1.883\left(\frac{\rho}{\rho_{\text{ice}}}\right)^2 + 0.107\frac{\rho}{\rho_{\text{ice}}} + 0.0386 & \text{for T = 268 K} \\ 1.776\left(\frac{\rho}{\rho_{\text{ice}}}\right)^2 + 0.147\frac{\rho}{\rho_{\text{ice}}} + 0.0455 & \text{for T = 273 K} \end{cases} \quad (18)$$

where $\frac{\rho}{\rho_{\text{ice}}}$ is the volume fraction of ice and the constant terms in the polynomial equations correspond to k_{v}. Similar parametrizations for the horizontal thermal conductivity, and for the geometric mean of the vertical and horizontal thermal conductivities are available as a Supplementary Material. This parametrization can be extended to other temperatures by first computing the thermal conductivity at the desired density for the 5 proposed temperatures and then performing an interpolation to the desired temperature.

These vertical effective thermal conductivity parametrizations, displayed in Figure 9, show a ~~flattening of~~ decrease of the slopes of the thermal conductivity versus density ~~curve with increasing temperature~~curves with increasing temperatures. This is consistent with the observations made in Section 3.1, that the thermal conductivity of the low-density sample increases with

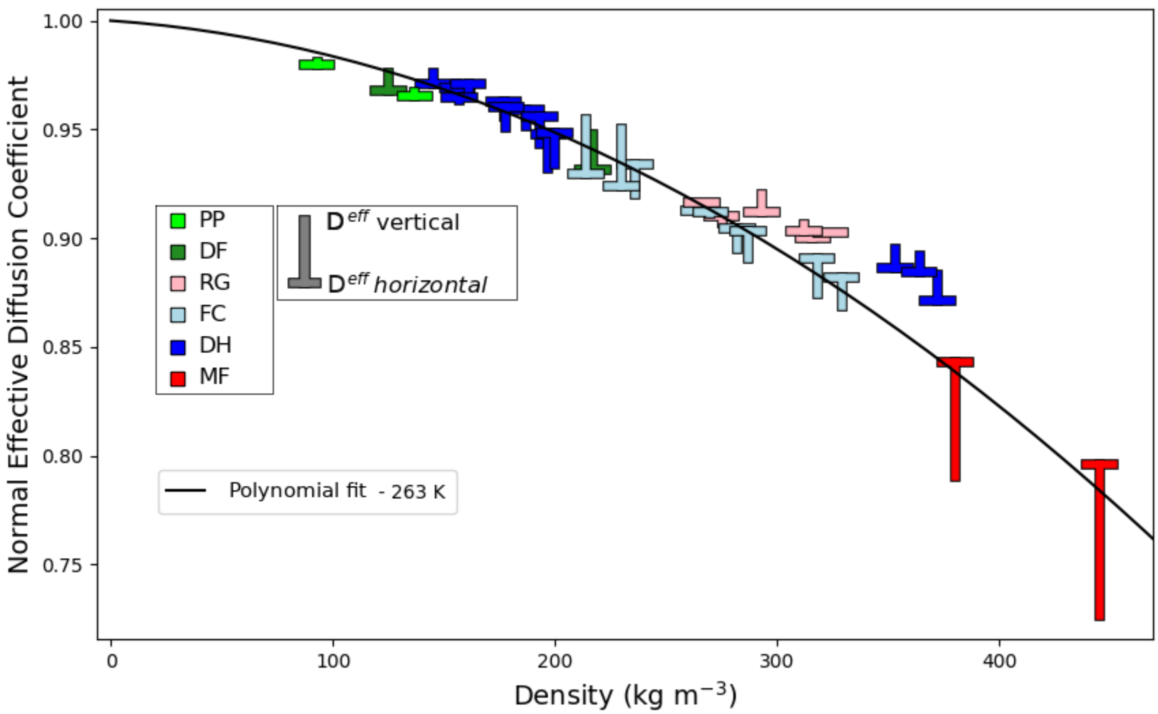

Figure 10. Normalized effective diffusion coefficient as a function of density, under the fast kinetics assumption at 263 K. Snow classification according to Fierz et al. (2009). Solid black line: normalized effective diffusion coefficient deduced from the application of Equation 14 with the effective thermal conductivity polynomial fit of Figure 8.

temperature while the thermal conductivity of the high-density sample decreases with temperature. The transition between these two behaviors lies around 350 to $400\,\mathrm{kg\,m^{-3}}$. Note that Calonne et al. (2019) report that a similar transition between the low and high-density samples also exists under limited kinetics, but occurs at a much lower density of about $100\,\mathrm{kg\,m^{-3}}$.

Finally, the estimated normalized effective diffusion coefficients of water vapor are displayed in Figure 10 as a function of density at $263\,\mathrm{K}$. The normalized effective diffusion coefficients obtained by application of Equation 14 together with the polynomial fit of the vertical effective thermal conductivity are shown as a black solid line in Figure 10. The normalized effective diffusion coefficient decreases with density and mostly remains in the 0.98 to 0.8 range. Notably, detailed seasonal snow models working under the fast kinetics assumption could thus make the reasonable simplifying assumption that $D^{\mathrm{norm}} = 0.90$, independent of snow type. This would result in a less than $10\,\%$ error on the effective diffusion coefficient of water vapor.

4 Discussion

4.1 Does the fast kinetics hypothesis apply for heat and mass transport in snow?

This paper studied two limiting cases, considering either the kinetics of water vapor deposition/sublimation to be sufficiently fast to impose saturated water vapor at the ice interface (very large α) or that the kinetics is sufficiently slow so that latent heat does not impact ~~the temperature and thus~~ either the temperature gradients nor the heat conduction in the snow microstructure (very small α). It remains however unclear if one of these two limiting cases applies for snow modeling. For ~~instance~~example, based on the observation of snow crystal growth with computed tomography, Krol and Löwe (2016) suggest that isothermal metamorphism is slightly better represented by a slow kinetics, while temperature gradient metamorphism data appear consistent with fast kinetics.

As seen in Section 3.1, the effective thermal conductivity of low-density snow displays a fundamentally different dependence on temperature, depending on whether the slow or the fast kinetics hypothesis applies. In the slow kinetics case, the effective thermal conductivity slightly decreases with increasing temperature, while it increases in the fast kinetics case. Using the needle probe method, Sturm and Johnson (1992) measured the variation of the effective thermal conductivity of a low-density sample of depth hoar with temperature. Even though recent studies have highlighted a potential bias of the needle probe method when used with snow (Calonne et al., 2011; Riche and Schneebeli, 2013), ~~we can expect the variations with temperature measured by Sturm and Johnson (1992) to be reflective of the real~~ this reported bias does not impact the trend of thermal conductivity measured at different temperature in similar snow samples, as performed by Sturm and Johnson (1992). These data can thus be expected to reflect the variation of the effective thermal conductivity with temperature. These measurements, displayed in Figure 7 of Sturm and Johnson (1992), clearly indicate an exponential-like increase of thermal conductivity with temperature, consistent with the fast kinetics hypothesis but not with the slow kinetics hypothesis.

The differences between the slow and fast kinetics cases on the effective diffusion coefficient of water vapor were also studied by Fourteau et al. (2021). While direct measurements of the effective diffusion coefficient are difficult and should therefore be analyzed with caution, the reported experimental values ~~systematically show a diffusivity of water vapor in snow much higher than what would be expected for slow kinetics, and more consistent with the fast kinetics case. Notably, the experimental study~~ of Sokratov and Maeno (2000) reports an average normalized diffusion coefficient of 0.64 for snow densities of about $475\,\mathrm{kg\,m^{-3}}$, while Calonne et al. (2014) report a value of about 0.35 for limited kinetics and extrapolation of our results suggests a value of about 0.70 under the fast kinetics. Finally, the numerical simulations of Fourteau et al. (2021) indicates that for water vapor diffusion the transition between the slow and fast kinetics regimes occurs for sticking coefficients α around 10^{-3}. Based on data by Libbrecht (2006), Kaempfer and Plapp (2009) reports that α is likely to be within the 10^{-3} to 10^{-1} range, thus within the fast kinetics regime.

All the above reasons suggest that the effective thermal conductivity and diffusion coefficient of water vapor in snow could be well represented under the fast kinetics hypothesis, at least during ~~thermal~~ temperature gradient metamorphism. ~~That being said, further work remains required before robustly accessing whether~~ Further experimental work should be performed to confirm that the fast kinetics assumption generally applies for modeling mass and heat transport in snow ~~should be treated~~

~~using the slow kineticshypothesis, the fast kinetics hypothesis, or an intermediate case~~and to highlight its potential limitations. Also, the derivation of a theoretical model able to describe heat and mass transfer with arbitrary surface kinetics would allow to investigate intermediate kinetics, in an effort to ultimately select the best modeling assumptions for snow. At the same time, this model could be formulated to explicitly take into account macroscopic convection, as this phenomenon has been observed in sub-artic shallow snowpacks (Trabant and Benson, 1972; Sturm and Johnson, 1991). Its derivation could be achieved using standard homogenization methods, such as the two-scale asymptotic expansion (e.g. Municchi and Icardi, 2020) or volume averaging methods (e.g. Whitaker, 1977).

4.2 The coupling of heat conduction with vapor transport

We showed that in the fast kinetics case, the pure conduction part $\mathbf{K}^{\mathrm{cond}}$ of the effective thermal conductivity is influenced by the presence of water vapor and its latent heat. Therefore, the definition of $\mathbf{K}^{\mathrm{cond}}$ given by Sturm and Johnson (1992), i.e. that it is*"the hypothetical conductivity in the absence of any vapor transport"*, should be clarified to emphasize that $\mathbf{K}^{\mathrm{cond}}$ corresponds to the pure conduction ~~occuring~~ occurring through the ice and pore spaces, but ~~with the~~ in response to the actual microscopic thermal gradients ~~taking into account water vapor latent heat~~ that are influenced by the latent heat effects. Furthermore, the dependence of the pure conduction part on temperature is different from what would be expected from variations of the ice and air thermal conductivity only. This means that under the fast kinetics hypothesis a strong two-way coupling exists between heat conduction and water vapor transport, and the heat conduction process cannot be fully considered without latent heat processes. One should therefore be careful when treating heat conduction as decoupled from vapor transport (e.g. Calonne et al., 2011; Riche and Schneebeli, 2013). While this approximation is justified if the effects of latent heat are small, one should be aware of the potential limit of this approximation. Finally, in such a case it is not possible to experimentally decouple the measurement of $\mathbf{K}^{\mathrm{cond}}$ from $\mathbf{K}^{\mathrm{vap}}$ by performing measurements at low temperature (where $\mathbf{K}^{\mathrm{vap}} \simeq 0$). The inferred value of $\mathbf{K}^{\mathrm{cond}}$ at low-temperature does not hold at higher temperatures, where the effect of latent heat is no longer negligible and thus impacts $\mathbf{K}^{\mathrm{cond}}$. A similar conclusion was reached by Moyne et al. (1988) for the thermal conductivity of humid ~~soils~~tri-phasic medium.

5 Conclusions

This paper investigates the effective thermal conductivity of snow and its relationship to the diffusion of water vapor and its associated latent heat. Using theory, we show that the kinetics of the sublimation and deposition processes at the ice surfaces plays a significant role on the transport of heat in snow. In particular, if the kinetics is slow we recall that snow can be treated as an inert medium and that heat transport only occurs through conduction in the ice and in the air. In contrast, if the kinetics is fast vapor transport and latent heat effects become an integral part of heat transport, and the effective thermal conductivity of snow is composed of a purely conductive term and a term proportional to the water vapor diffusivity. Moreover, we show that under the latter hypothesis there is a simple linear relationship between the effective diffusion coefficient of water vapor in snow and the effective thermal conductivity. Since the effective thermal conductivity of snow rarely exceeds $0.5\,\mathrm{W\,K^{-1}\,m^{-1}}$, we conclude that under fast kinetics the normalized effective diffusion coefficient of water vapor ranges between 1 to about 0.80 for most seasonal snow.

We complemented this theoretical work by Finite Elements simulations of heat conduction through snow microstructures obtained with computed tomography. The simulations were performed on a total of 34 samples, covering the typical seasonal snow types, under both the slow and fast kinetics hypotheses, and for temperatures ranging from 223 to $273\,\mathrm{K}$. The simulations were performed on large samples, in order to ensure the ~~representativity~~ representativeness of the results.

Using this new set of numerical simulations, we show that the influence of vapor transport in the fast kinetics case can lead to a significant increase of the effective thermal conductivity compared to the slow kinetics case, up to 50% for low-density snow near the melting point. Moreover, we show that under the fast kinetics hypothesis the purely conductive term of the effective thermal conductivity is influenced by the presence of water vapor, and differs from the effective thermal conductivity in the absence of any vapor transport. Indeed, sublimation and deposition processes modify the ice surface temperature through latent heat effect, therefore affecting thermal gradients throughout the snow microstructure. This observation illustrates the coupled nature of heat and water vapor transport in snow, where one cannot be fully understood and quantified without the other. We also compared our numerical simulations to published experimental data of the dependence of the effective thermal conductivity of snow on temperature. This suggests that the fast kinetics option might be well suited to model ~~snow~~heat and mass transport in snow during temperature gradient metamorphism.

Finally, we provide our new numerical values of the effective thermal conductivity and of the effective diffusion coefficient of water vapor under the fast kinetics hypothesis, derived from snow microstructures measured with computed tomography, as well as parametrizations with snow density. These new data and parametrizations are primarily meant to be used ~~by~~ in detailed snow physics ~~model~~models.

Code availability. The codes for the numerical simulations and their analysis will be provided upon direct request to the corresponding author.

Author contributions. The research was designed by FD, KF and PH. FD obtained funding. KF performed research and wrote the paper with inputs from FD and PH.

Competing interests. The authors declare having no competing interests.

Acknowledgements. This work contributes to the APT project (Acceleration of Permafrost Thaw), funded by the Climate Initiative program of the BNP-Paribas Foundation. We acknowledge Marion Reveillet, Marie Dumont, François Tuzet, Neige Calonne, Anne Dufour and the ANR JCJC EBONI (grant no. ANR-16-CE01-006) for providing the tomography scan of a Melt Form sample. The rest of the unpublished samples were obtained thanks to the help of Jacques Roulle and the tomography apparatus with funding from the INSU-LEFE, the LabEx OSUG and the CNRM. We thank Neige Calonne and Marie Dumont for their valuable inputs on the article. We are thankful to Charles Fierz and the two anonymous reviewers for reviewing the manuscript, and to Carrie Vuyovich for editing it.

References

Auriault, J.: Heterogeneous medium. Is an equivalent macroscopic description possible?, International J. Engin. Sci., 29, 785–795, https://doi.org/10.1016/0020-7225(91)90001-J, 1991.

Auriault, J.-L., Boutin, C., and Geindreau, C.: Homogenization of coupled phenomena in heterogenous media, vol. 149, John Wiley & Sons, 2010.

Batchelor, G. K. and Brien, R. W.: Thermal or electrical conduction through a granular material, Proc. Royal Soc. Lond. A. Math. Phys. Sci., 355, 313–333, https://doi.org/10.1098/rspa.1977.0100, 1977.

Calonne, N., Flin, F., Morin, S., Lesaffre, B., du Roscoat, S. R., and Geindreau, C.: Numerical and experimental investigations of the effective thermal conductivity of snow, Geophys. Res. Lett., 38, L23 501, https://doi.org/10.1029/2011GL049234, 2011.

Calonne, N., Geindreau, C., and Flin, F.: Macroscopic modeling for heat and water vapor transfer in dry snow by homogenization, J. Phys. Chem. B, 118, 13 393–13 403, https://doi.org/10.1021/jp5052535, 2014.

Calonne, N., Milliancourt, L., Burr, A., Philip, A., Martin, C. L., Flin, F., and Geindreau, C.: Thermal Conductivity of Snow, Firn, and Porous Ice From 3-D Image-Based Computations, Geophys. Res. Let., 46, 13 079–13 089, https://doi.org/10.1029/2019GL085228, 2019.

Colbeck, S. C.: An overview of seasonal snow metamorphism, Revi. Geophys., 20, 45–61, https://doi.org/10.1029/RG020i001p00045, 1982.

Colbeck, S. C.: Theory of metamorphism of dry snow, J. Geophys. Res. Oceans, 88, 5475–5482, https://doi.org/10.1029/JC088iC09p05475, 1983.

Colbeck, S. C.: The vapor diffusion coefficient for snow, Water Resour. Res., 29, 109–115, https://doi.org/10.1029/92WR02301, 1993.

De Vries, D. A.: Simultaneous transfer of heat and moisture in porous media, Eos, Trans. Am. Geophys. Union, 39, 909–916, https://doi.org/10.1029/TR039i005p00909, 1958.

De Vries, D. A.: The theory of heat and moisture transfer in porous media revisited, Int. J. Heat Mass Transf., 30, 1343–1350, https://doi.org/10.1016/0017-9310(87)90166-9, 1987.

Domine, F., Barrere, M., Sarrazin, D., Morin, S., and Arnaud, L.: Automatic monitoring of the effective thermal conductivity of snow in a low-Arctic shrub tundra, The Cryosphere, 9, 1265–1276, https://doi.org/10.5194/tc-9-1265-2015, 2015.

Domine, F., Picard, G., Morin, S., Barrere, M., Madore, J.-B., and Langlois, A.: Major Issues in Simulating Some Arctic Snowpack Properties Using Current Detailed Snow Physics Models: Consequences for the Thermal Regime and Water Budget of Permafrost, J. Adv. Model. Earth Syst., 11, 34–44, 2019.

Fierz, C., Armstrong, R. L., Durand, Y., Etchevers, P., Greene, E., McClung, D. M., Nishimura, K., Satyawali, P. K., and Sokratov, S. A.: The International Classificationi for Seasonal Snow on the Ground, 2009.

Fourteau, K., Domine, F., and Hagenmuller, P.: Macroscopic water vapor diffusion is not enhanced in snow, The Cryosphere, 15, 389–406, https://doi.org/10.5194/tc-15-389-2021, 2021.

Giddings, J. C. and LaChapelle, E.: The formation rate of depth hoar, J. Geophys. Res., 67, 2377–2383, https://doi.org/10.1029/JZ067i006p02377, 1962.

Gilbert, A., Vincent, C., Wagnon, P., Thibert, E., and Rabatel, A.: The influence of snow cover thickness on the thermal regime of Tête Rousse Glacier (Mont Blanc range, 3200 m asl): Consequences for outburst flood hazards and glacier response to climate change, J. Geophys. Res.: Earth Surf., 117, 2012.

Hagenmuller, P., Matzl, M., Chambon, G., and Schneebeli, M.: Sensitivity of snow density and specific surface area measured by microtomography to different image processing algorithms, The Cryosphere, 10, 1039–1054, https://doi.org/10.5194/tc-10-1039-2016, 2016.

Hagenmuller, P., Flin, F., Dumont, M., Tuzet, F., Peinke, I., Lapalus, P., Dufour, A., Roulle, J., Pézard, L., Voisin, D., Ando, E., Rolland du Roscoat, S., and Charrier, P.: Motion of dust particles in dry snow under temperature gradient metamorphism, The Cryosphere, 13, 2345–2359, https://doi.org/10.5194/tc-13-2345-2019, 2019.

Hansen, A. C. and Foslien, W. E.: A macroscale mixture theory analysis of deposition and sublimation rates during heat and mass transfer in dry snow, The Cryosphere, 9, 1857–1878, https://doi.org/10.5194/tc-9-1857-2015, 2015.

Jaafar, H. and Picot, J. J. C.: Thermal conductivity of snow by a transient state probe method, Water Resour. Res., 6, 333–335, https://doi.org/10.1029/WR006i001p00333, 1970.

Jordan, R.: A one-dimensional temperature model for a snow cover: Technical documentation for SNTHERM. 89., Tech. rep., Cold Regions Research and Engineering Lab Hanover NH, 1991.

Kadoya, K., Matsunaga, N., and Nagashima, A.: Viscosity and Thermal Conductivity of Dry Air in the Gaseous Phase, J. Phys. Chem. Ref. Data, 14, 947–970, https://doi.org/10.1063/1.555744, 1985.

Kaempfer, T. U. and Plapp, M.: Phase-field modeling of dry snow metamorphism, Phys. Rev. E, 79, 031 502, https://doi.org/10.1103/PhysRevE.79.031502, 2009.

Krol, Q. and Löwe, H.: Analysis of local ice crystal growth in snow, J. Glaciol., 62, 378–390, https://doi.org/10.1017/jog.2016.32, 2016.

Lecomte, O., Fichefet, T., Vancoppenolle, M., Domine, F., Massonnet, F., Mathiot, P., Morin, S., and Barriat, P.-Y.: On the formulation of snow thermal conductivity in large-scale sea ice models, J. Adv. Model. Earth Syst., 5, 542–557, 2013.

Legagneux, L. and Domine, F.: A mean field model of the decrease of the specific surface area of dry snow during isothermal metamorphism, J. Geophys. Res. Earth Surf., 110, https://doi.org/10.1029/2004JF000181, 2005.

Libbrecht, K. G.: Precision Measurements of Ice Crystal Growth Rates, Tech. rep., Department of Physics, California Institute of Technology, Pasadena, California 91125, US, 2006.

Libbrecht, K. G. and Rickerby, M. E.: Measurements of surface attachment kinetics for faceted ice crystal growth, J. Crystal Growth, 377, 1–8, https://doi.org/10.1016/j.jcrysgro.2013.04.037, 2013.

Lide, D. R.: CRC handbook of chemistry and physics, chap. Properties of ice and supercooled water, pp. 6–5, CRC press, Taylor and Francis, Boca Raton, FL, 85 edn., 2006.

Löwe, H., Riche, F., and Schneebeli, M.: A general treatment of snow microstructure exemplified by an improved relation for thermal conductivity, The Cryosphere, 7, 1473–1480, https://doi.org/10.5194/tc-7-1473-2013, 2013.

Malinen, M. and Råback, P.: Elmer Finite Element Solver for Multiphysics and Multiscale Problems, in: Multiscale Modelling Methods for Applications in Materials Science, edited by Kondov, I. and Sutmann, G., pp. 101–113, Forschungszentrum Jülich GmbH, 2013.

Morin, S., Domine, F., Arnaud, L., and Picard, G.: In-situ monitoring of the time evolution of the effective thermal conductivity of snow, Cold Reg. Sci. Tech., 64, 73–80, https://doi.org/10.1016/j.coldregions.2010.02.008, 2010.

Moyne, C., Batsale, J.-C., and Degiovanni, A.: Approche expérimentale et théorique de la conductivité thermique des milieux poreux humides—II. Théorie, Int. J. Heat Mass Transf., 31, 2319–2330, https://doi.org/10.1016/0017-9310(88)90163-9, 1988.

Municchi, F. and Icardi, M.: Macroscopic models for filtration and heterogeneous reactions in porous media, Adv. Water Resour., 141, 103 605, https://doi.org/10.1016/j.advwatres.2020.103605, 2020.

Peinke, I., Hagenmuller, P., Andò, E., Chambon, G., Flin, F., and Roulle, J.: Experimental Study of Cone Penetration in Snow Using X-Ray Tomography, Front. Earth Sci., 8, 63, https://doi.org/10.3389/feart.2020.00063, 2020.

Pinzer, B. R., Schneebeli, M., and Kaempfer, T. U.: Vapor flux and recrystallization during dry snow metamorphism under a steady temperature gradient as observed by time-lapse micro-tomography, The Cryosphere, 6, 1141–1155, https://doi.org/10.5194/tc-6-1141-2012, 2012.

Riche, F. and Schneebeli, M.: Thermal conductivity of snow measured by three independent methods and anisotropy considerations, The Cryosphere, 7, 217–227, https://doi.org/10.5194/tc-7-217-2013, 2013.

Saito, Y.: Statistical physics of crystal growth, World Scientific, 1996.

Shertzer, R. H. and Adams, E. E.: A Mass Diffusion Model for Dry Snow Utilizing a Fabric Tensor to Characterize Anisotropy, J Adv. Model. Earth Sys., 10, 881–890, https://doi.org/10.1002/2017MS001046, 2018.

Slack, G. A.: Thermal conductivity of ice, Phys. Rev. B, 22, 3065–3071, https://doi.org/10.1103/PhysRevB.22.3065, 1980.

Sokratov, S. A. and Maeno, N.: Effective water vapor diffusion coefficient of snow under a temperature gradient, Water Resour. Res., 36, 1269–1276, https://doi.org/10.1029/2000WR900014, 2000.

Sommerfeld, R. A. and LaChapelle, E.: The Classification of Snow Metamorphism, J. Glaciol., 9, 3–18, https://doi.org/10.3189/S0022143000026757, 1970.

Sturm, M. and Benson, C. S.: Vapor transport, grain growth and depth-hoar development in the subarctic snow, J. Glaciol., 43, 42–59, https://doi.org/10.3189/S0022143000002793, 1997.

Sturm, M. and Johnson, J. B.: Natural convection in the subarctic snow cover, J. Geophys. Res. Solid Earth, 96, 11 657–11 671, https://doi.org/10.1029/91JB00895, 1991.

Sturm, M. and Johnson, J. B.: Thermal conductivity measurements of depth hoar, J. Geophys. Res. Solid Earth, 97, 2129–2139, https://doi.org/10.1029/91JB02685, 1992.

Sturm, M., Holmgren, J., König, M., and Morris, K.: The thermal conductivity of seasonal snow, J Glaciol., 43, 26–41, https://doi.org/10.3189/S0022143000002781, 1997.

Trabant, D. and Benson, C.: Field experiments on the development of depth hoar, Geol. Soc. Am. Mem., 135, 309–322, 1972.

Vionnet, V., Brun, E., Morin, S., Boone, A., Faroux, S., Le Moigne, P., Martin, E., and Willemet, J.-M.: The detailed snowpack scheme Crocus and its implementation in SURFEX v7.2, Geosci. Mod. Devel., 5, 773–791, https://doi.org/10.5194/gmd-5-773-2012, 2012.

Whitaker, S.: Simultaneous Heat, Mass, and Momentum Transfer in Porous Media: A Theory of Drying, 13, 119–203, https://doi.org/10.1016/S0065-2717(08)70223-5, 1977.

Yosida, Z., Oura, H., Kuroiwa, D., Huzioka, T., Kojima, k., Aoki, S.-I., and Kinosita, S.: Physical Studies on Deposited Snow. I. Thermal Properties., Contributions from the Institute of Low Temperature Science, 7, 19–74, 1955.

Zhang, T., Osterkamp, T. E., and Stamnes, K.: Influence of the depth hoar layer of the seasonal snow cover on the ground thermal regime, Water Resour. Res., 32, 2075–2086, 1996.